

AD-A022 351

IMPACT PULSE SHAPING

Irvin Pollin

Harry Diamond Laboratories
Adelphi, Maryland

June 1975

DISTRIBUTED BY:

NTIS

National Technical Information Service
U. S. DEPARTMENT OF COMMERCE

REPRODUCED BY
**NATIONAL TECHNICAL
INFORMATION SERVICE**
U. S. DEPARTMENT OF COMMERCE
SPRINGFIELD, VA. 22161

UNCLASSIFIED

SECURITY CLASSIFICATION OF THIS PAGE (When Data Entered)

REPORT DOCUMENTATION PAGE		READ INSTRUCTIONS BEFORE COMPLETING FORM
1. REPORT NUMBER HDL-TR-1710	2. JOVT ACCESSION NO.	4. RECIPIENT'S CATALOG NUMBER
4. TITLE (and Subtitle) Impact Pulse Shaping		5. TYPE OF REPORT & PERIOD COVERED Technical Report
7. AUTHOR(s) Irvin Pollin		6. PERFORMING ORG. REPORT NUMBER
9. PERFORMING ORGANIZATION NAME AND ADDRESS Harry Diamond Laboratories 2800 Powder Mill Road Adelphi, MD 20783		8. CONTRACT OR GRANT NUMBER(s)
11. CONTROLLING OFFICE NAME AND ADDRESS Commander, U S Army Materiel Command 5001 Eisenhower Avenue Alexandria, VA 22333		10. PROGRAM ELEMENT, PROJECT, TASK AREA & WORK UNIT NUMBERS Prog Ele 6.11.01A
14. MONITORING AGENCY NAME & ADDRESS (if different from Controlling Office)		12. REPORT DATE June 1975
		13. NUMBER OF PAGES 59
		15. SECURITY CLASS. (of this report) Unclassified
		16a. DECLASSIFICATION/DOWNGRADING SCHEDULE
16. DISTRIBUTION STATEMENT (of this Report) Approved for public release; distribution unlimited.		
17. DISTRIBUTION STATEMENT (of the abstract entered in Block 20, if different from Report) D D C RECEIVED MAR 29 1976		
18. SUPPLEMENTARY NOTES HDL Project No. A10586 AMCMS Code: 6111011184400		
19. KEY WORDS (Continue on reverse side if necessary and identify by block number) Honeycomb Setback acceleration Mitigator Projectiles Impact Gun interior ballistics Pulse shaping Artillery simulation		
20. ABSTRACT (Continue on reverse side if necessary and identify by block number) The Harry Diamond Laboratories 4- and 7-in. air guns are used to slowly accelerate projectiles and components contained therein to speeds up to 900 ft/sec. The impacts of these projectiles are designed to produce pulse shapes (projectile decelerations) that simulate the interior ballistic acceleration environments occurring in a real gun. The continuity, momentum, and energy conservation equations are applied to the impact testing of projectiles, and calculations obtained therefrom are compared with experimental air		

UNCLASSIFIED

SECURITY CLASSIFICATION OF THIS PAGE(When Data Entered)

gun data of projectile time-deceleration. Data refer to projectile speeds of 300 to 650 ft/sec, accelerations up to 40,000 g, with energies of 14,000 and 43,000 ft-lb (for the 4- and 7-in. guns, respectively) impacting on aluminum honeycomb mitigators having a variable crush area, uniform static crush strengths of 725, 2000, 4000, and 8000 psi, and a velocity (strain-rate) dependent dynamic crush strength.

Within the limits of the projectile energy, mass, and available mitigator strengths, it is shown that the entire pulse shape can be controlled by shaping the crush area of the mitigator and by use of stock-item railroad springs. The mitigator shape controls the pulse rise and steady parts, and the springs control the pulse fall. Moreover, it is shown that high transient stress wave effects produced by impact can be eliminated from the pulse by shaping the mitigator and by the use of springs, thereby attaining a very smooth pulse.

UNCLASSIFIED

SECURITY CLASSIFICATION OF THIS PAGE(When Data Entered)

TABLE OF CONTENTS

	<u>Page</u>
1. INTRODUCTION	7
2. MITIGATOR AND MEM DESIGNS	9
3. CONSERVATION EQUATIONS	14
3.1 Mass Conservation	14
3.2 Momentum Conservation	14
3.3 Energy Conservation	18
4. COMPUTER PROGRAMS	19
4.1 VARYB	20
4.2 PULSE1	20
4.3 PULSE3	21
4.4 JMEM and JBIRD	21
5. THEORETICAL AND EXPERIMENTAL RESULTS	22
5.1 Conical Shaped Mitigator on the Bird with a Mass MEM	25
5.2 Conical Shaped Mitigator on the Bird with the Spring MEM.	30
5.3 Wedge Mitigator on the Bird with a Spring MEM	36
5.4 Mitigator Placed Adjacent to Spring MEM	37
5.5 Additional Data	39
6. SUMMARY AND CONCLUSIONS	41
7. LIST OF SYMBOLS	43
8. CODES	46
ACKNOWLEDGEMENT	58
DISTRIBUTION	59

LIST OF ILLUSTRATIONS

Figure

1	Impact components	8
2	Shaped mitigator crush	10
3	Flat-faced mitigator crush	11
4	Conical mitigator	11

LIST OF ILLUSTRATIONS (CONT'D)

<u>Figure</u>		<u>Page</u>
5	Double wedge mitigator	12
6	Triple wedge mitigator	12
7	Spring MEM	13
8	Notation for shaped mitigator attached to bird with a mass MEM	20
9	Notation for shaped mitigator attached to bird with spring MEM	21
10	Setback acceleration for flat-faced mitigator attached to bird with mass MEM	27
11a	Comparison of experimental and calculated setback accel- eration for conical mitigator attached to bird with mass MEM Shot 1703	29
11b	Comparison of experimental and calculated setback accel- eration for conical mitigator attached to bird with mass MEM Shot 1709	29
12a	Comparison of experimental and calculated setback accel- eration of 7 shots for conical mitigator attached to bird with spring MEM TC=665	32
12b	Calculated setback acceleration for conical mitigator attached to bird with spring MEM for various dynamic crush strengths TC=665	33
13a	Comparison of experimental and calculated setback accel- eration of 7 shots for conical mitigator attached to bird with spring MEM TC=688	34
13b	Calculated setback acceleration for conical mitigator attached to bird with spring MEM for various dynamic crush strengths TC=688	35
14	Comparison of experimental and calculated setback accel- eration for double wedge mitigator attached to bird with spring MEM	37
15	Comparison of experimental and calculated setback accel- eration for double-wedge mitigator attached to spring MEM	38

LIST OF ILLUSTRATIONS (CONT'D)

<u>Figure</u>		<u>Page</u>
16a	Comparison of experimental and calculated setback acceleration in the 7-in. gun for double-wedge honeycomb mitigator attached to mass MEM	40
16b	Comparison of experimental and calculated setback acceleration for double-wedge honeycomb mitigator attached to infinite mass MEM	40
17	Comparison of experimental and calculated setback acceleration for double-wedge honeycomb mitigator attached to bird with mass MEM	41
18	Comparison of experimental and calculated setback acceleration for double-wedge honeycomb mitigator attached to bird with spring MEM	42

LIST OF TABLES

<u>Table</u>		
I	Summary of Calculated Forces and Motions of System Components for Conical Mitigator Attached to Bird, with Spring MEM	23
II	Summary of Calculated Forces and Motions of System Components for Double-wedge Mitigator Attached to Bird, with Spring MEM	26
III	Summary of Calculated Forces and Motions of System Components for Double-wedge Mitigator Attached to MEM, with Spring MEM	26

1. INTRODUCTION

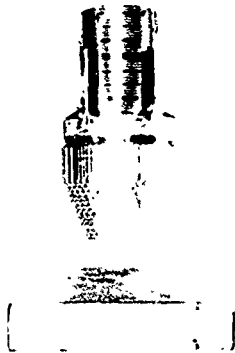
The Harry Diamond Laboratories 4- and 7-in.-diameter x 90-ft-length gas guns are used to provide a simulation of artillery interior ballistic acceleration environments of ordnance projectiles. In this simulation, the projectile (called a bird), having equipment on board to be test-evaluated, emerges from the muzzle of the 4- or 7-in. gun with an energy of 14,000 or 43,000 ft-lb, respectively, and with speeds up to 900 ft/sec. The equipment in the bird is mounted so that the acceleration force (pulse) on impact is in the same direction as the acceleration force (setback) in the weapon. The pulse is caused by the crushing of an aluminum honeycomb* mitigator, located between the bird and a momentum exchange mass (MEM), which is at rest before impact. The mitigator can either be launched to move with the bird (in which case it is attached to the bird nose), or may be attached to the MEM (fig. 1). For a nonelastic MEM, the ratio of MEM to mitigator masses is of the order 100, and the ratio of MEM to bird masses is of the order 10. The test simulation is designed so that the terminal velocity of the bird is approximately zero and its entire momentum is transferred to the MEM or to the mitigator and MEM. A description of the gas gun facility and its operation is given by H. D. Curchack.¹

The pulse experienced by the bird is comprised of essentially three parts: rise, steady, and fall. The rise and steady parts occur during the crushing of the mitigator, and their characteristic features are determined primarily by the bird mass and the dynamic crush strength of the mitigator. In addition, particularly at high crush speeds, the acceleration of the crushed mitigator, and thereby the mitigator density, affects the bird deceleration when the mitigator is attached to the MEM. As will be shown, aluminum honeycomb mitigators can be designed to provide a range of smooth rise and steady decelerations, consistent with the impact energy and mass of the bird. The fall characteristics depend on the bird and MEM masses and the elasticity of the system, namely, the elasticity of the mitigator and the springs provided in the MEM. Accordingly, the pulse fall can also be varied so that a wide range of pulse shapes can be obtained.

The conservation equations of mass, momentum, and energy are given for determining the forces acting on and the motions of the individual system components as functions of time. A comparison of experimental and calculated data is presented to indicate the validity of the theory.

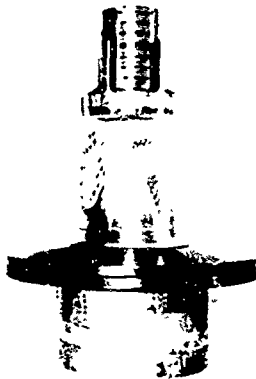
¹H. D. Curchack, Artillery Simulator for Fuze Evaluation. Shock and Vibration Bulletin (Dec 1970). Also reported in Harry Diamond Laboratories TR-1330 (Nov 1966).

*Aluminum honeycomb is also commercially available under such trade names as tubecore, spiralgrid, etc.



Negative No. 49-186-835 1974

a. Conical mitigator attached to bird with mass MEM.



Negative No. 49-186-833 1974

b. Bird and double wedge mitigator attached to spring MEM.

Figure 1. Impact Components

2. MITIGATOR AND MEM DESIGNS

Aluminum honeycomb is cellular in structure and the crushing occurs in cellular columns. Experimental data show that shear forces developed between crushed and uncrushed parts are insignificant in comparison with the static and dynamic crush forces.

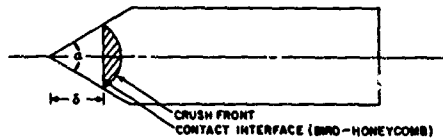
For a crush at the bird interface, the crushed material lies in the region bounded by the crush front and the flat nose of the bird. Referring to figures 2a and 3a, the bird has penetrated the mitigator by the distance δ and the shaded region denotes the crushed material. Since the honeycomb structure is uniform across the section, the crush front is always planar for a mitigator whose area remains constant during the crush, figure 3a. For the mitigator having the triangular-shaped section shown in figure 2a, because of the column-like crush, the crush front is not planar but is fully determined by the vertex angle α , the bird penetration δ , and the mass densities of the crushed and uncrushed material. To attain a continuously smooth pulse, the mitigator is designed so that the instantaneous crush takes place at the weakest section and progresses continuously toward the stronger sections. To this end, the mitigator section area is made a monotonic nondecreasing function of the bird penetration, and the instantaneous effective mitigator crush area is the instantaneous mitigator face area with the bird. Experiments show that the initial crush force is about 50 percent larger for an uncrushed mitigator than one for which some crush has occurred. Thus, experiments show that the crush continues only at the shaped end of the mitigator, even after the instantaneous crush area becomes equal to that of the unshaped face (fig. 2b). However, the crush generally occurs at both ends of a flat-faced mitigator.

For a crush at the MEM interface and penetration only by the MEM, the above description remains the same, except that the mitigator has been turned around (so that its weakest section faces the MEM) and moves with the bird in the gun, figure 3b.

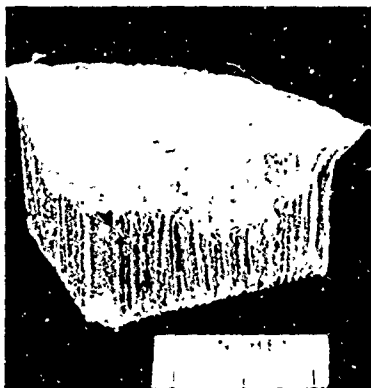
In practice, mitigators with an axisymmetric nose cannot be used because the mitigator and bird center-of-mass axes will not perfectly coincide and the bird will tend to tumble as it impacts. Consequently, for stability, mitigators shaped with off-axis nose projections are used, figures 4, 5, and 6.

In the following presentation, the length of the shaped end in the direction of the bird motion is called the altitude length and the remaining length in this direction is called the base length.

The dynamic crush force of the aluminum honeycomb is significantly larger than the static crush force and was determined empirically. For a given bird mass, the rise and steady parts of the pulse can be



a. Schematic.



Negative No. 49-186-837 1974

b. Crush of conical mitigator

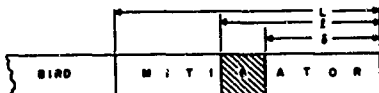
Figure 2. Shaped mitigator crush.

designed by shaping the mitigator; i.e., the crush area is a designed function of the bird or MEM penetration and the bird speed relative to the MEM. The mitigator is always long enough to avoid complete crushing or "bottoming," since the forces at "bottoming" greatly exceed the dynamic crush force.

The mitigator retains elastic energy when the bird speed relative to the MEM is zero. The amount of the associated compression displacement is small and thereby the fall time is short, typically about 100 usec when a pure mass MEM is used. The mass MEM is approximately 12 to 15 times larger than the total mass accelerated in the gun. The MEM mass is selected so that, together with the honeycomb elasticity, the terminal velocity of the bird will be approximately zero.

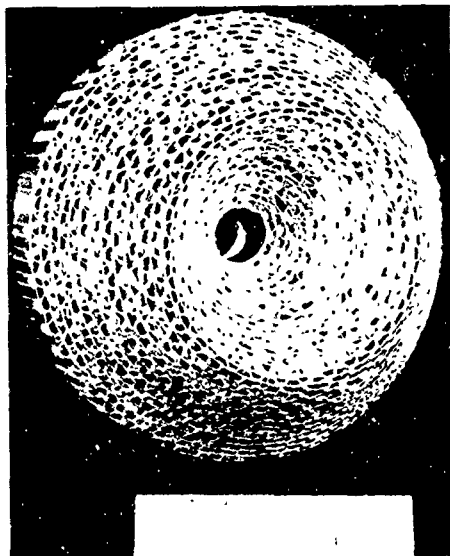


(a) Mitigator attached to PEN. Crush by bird penetration



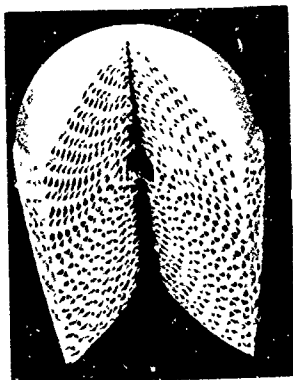
(b) Mitigator attached to bird. Crush by PEN penetration

Figure 3. Flat-faced mitigator crush.



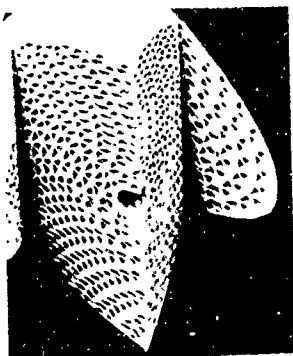
Negative No. 49-186-838 1974

Figure 4. Conical mitigator.



Negative No. 49-186-840 1974

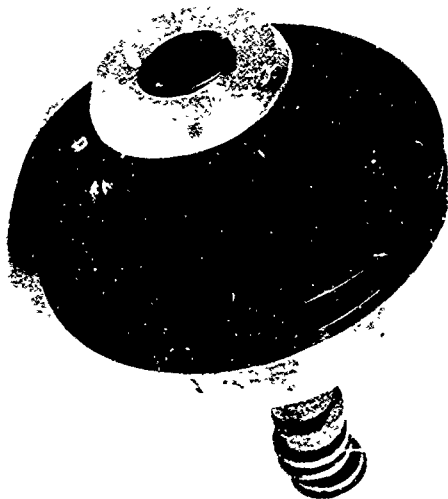
Figure 5. Double wedge mitigator.



Negative No. 49-185-839 1974

Figure 6. Triple wedge mitigator.

A spring MEM has been devised to obtain longer fall times and to allow for shaping the pulse fall (fig. 7). This MEM consists of a forward section, which makes the impact interface with the mitigator, two stock-item railroad springs, an aft section, and a washer, bushing, and connecting bolt to hold the device together. The device is free to compress, but cannot "fly" apart following impact because of the bolt action. In a typical shot, the two railroad springs, each weighing 5.3 lbs, provide a total stored energy corresponding to linear spring loading of 86,400 lbs and maximum deflection of 0.331 in. Typically, this stored energy provides for about a 300 μ sec fall time when the bird mass is 2000 grams and the peak bird deceleration exceeds 15,000 g. Smaller bird decelerations may not cause the full deflection of these springs and a reduced stored energy is available. Other fall times can be obtained by varying the bird, mitigator and MEM masses, varying the mitigator strength, and by changing the energy capacity of the springs.



Negative No. 49-186-834 1974

Figure 7. Spring MEM.

The above spring MEM is about one-half to one-third the weight of the pure mass MEM. Accordingly, the bird speed relative to the spring MEM becomes zero at a larger value of the bird speed relative to the gun. In practice, the fall time is limited by the fact that the final bird speed relative to the gun must be zero or slightly positive (i.e., the bird should not move backwards toward the gun and damage the payload). The acceleration-time function for the fall is fully determined by the physical constants.

3. CONSERVATION EQUATIONS

3.1 Mass Conservation

Referring to the sketch of the mitigator given in figure 3a, we assume that the mitigator is attached to the MEM and the crush proceeds from left to right. The original mitigator length is L, the bird has penetrated the mitigator by the distance δ and the crushed material is contained in the shaded space ($L - \delta$). Since the cross-sectional area is not significantly affected by the crush, mass conservation requires

$$\rho/\rho_1 = (S-1)/S, \quad (1)$$

where ρ and ρ_1 are the mass densities of the original mitigator and the crushed mitigator in the shaded region, and $S=L/\delta$.

3.2 Momentum Conservation

In deriving the momentum equation, we observe that the centers-of-mass for the crushed and uncrushed parts of the mitigator move at speeds which differ from U_1 and U_2 but depend on U_1 , U_2 , and S . Consequently, it appears necessary to derive a momentum equation from the relation expressing the center-of-gravity, \bar{Y} , of the entire moving system in terms of the centers-of-gravity, Y_I , of the system individual masses, M_I .* This is given by

$$M\bar{Y} = M_1Y_1 + M_2Y_2 + M_4Y_4 + M_5Y_5, \quad (2)$$

where

$$M = \sum_{I=1}^3 M_I.$$

*The author is especially indebted to H. D. Curchack of HDL for this consideration, the starting equation (2), and helpful discussions that resulted in equations 3(A) through 5(A).

Case A: Mitigator Adjacent To MEM And Mitigator Crushes At Bird Face.

The momentum of the system is $M1U0$, and time differentiation of equation (2) gives the momentum equation

$$M1U0 = M\dot{Y} = M1U1 + M2U2 + M4U4 + M5U5 + \dot{M}4(Y4-Y5). \quad (2A)$$

Referring to figure 3,

$$Y4 = (\ell + \delta)/2, \quad Y5 = (L + \ell)/2$$

$$\dot{\ell} = U2 + (U1 - U2)S, \quad \dot{\delta} = U1, \quad \dot{L} = U2$$

$$U4 = \frac{\dot{\ell} + \dot{\delta}}{2} = \frac{U1 + U2 + (U1 - U2)S}{2},$$

$$U5 = \frac{\dot{\ell} + \dot{L}}{2} = \frac{2U2 + (U1 - U2)S}{2},$$

$$\dot{M}4 = \rho A \dot{\ell}, \quad M5 = \rho A (L - \ell), \text{ and}$$

$$\dot{M}4 = \rho AS (U1 - U2) = \rho A (\dot{\ell} - \dot{L}).$$

Substituting the above quantities, we obtain

$$M4U4 + M5U5 + M4(Y4 - Y5) = \frac{M4(1-S)U2}{2} +$$

$$\frac{M4(1+S)U1}{2} + \frac{M5(2-S)U2}{2} + \frac{M5(S)U1}{2} +$$

$$\frac{\rho AS}{2} (U1 - U2) \{(\ell + \delta) - (L + \ell)\}.$$

Since $\rho AS (\delta - L) = -M4(S-1) - M5S$, there results

$$M4U4 + M5U5 + M4(Y4 - Y5) = M4U1 + M5U2, \text{ and the momentum}$$

equation becomes

$$M1U0 = \dot{M}Y = (M1+M4)U1 + (M2+M5)U2 . \quad (3A)$$

The momentum equation (3A) is exactly that which would result by assuming that the entire crushed and uncrushed masses move at speeds U1 and U2, respectively.

Since no external forces act on the system, time differentiation of equation (3A) gives

$$(M1+M4) A1 + (M2+M5) A2 + \dot{M}4 (U1-U2) = 0 . \quad (4A)$$

The forces transmitted to (M1+M4) and to (M2+M5) originate at the location l , see figure 3a. The time rate of change of mass, $\dot{M}4$, gives rise to a force acting on (M1+M4), so that

$$A1 = -(F+\dot{M}4(U1-U2))/(M1+M4) \quad (5A)$$

where F is the dynamic crush force of the mitigator. The value for F is generally a function of (U1-U2), and experiments using aluminum honeycomb indicate that F is larger than the static crush force, P. In addition, F varies linearly with the crush area normal to (U1-U2), and therefore also varies with the depth of penetration for shaped mitigators.

The only force that can be transmitted to (M2+M5) is F. Accordingly,

$$A2 = F/(M2+M5) . \quad (6A)$$

Case B: Mitigator Moves With Bird And Mitigator Crushes At MEM Face.

As in Case A, we start with the time derivative of equation (2). Since the mitigator moves with the bird, there results

$$(M1+M3) U0 = \dot{M}Y = M1U1 + M2U2 + M4U4 + M5U5 + \dot{M}4 (Y4-Y5) . \quad (2B)$$

Imagine that the entire mass system is subjected to a velocity $-U_0$; then the MEM and bird move to the left at speeds $U_2^1 = -U_0 + U_2$ and $U_1^1 = -U_0 + U_1$. The crush occurs at the MEM face and now proceeds from right to left. This crush is similar to that of Case A, where the crush occurs at the bird face and the crush proceeds from left to right. Since Y_4 , Y_5 , M_4 , M_4 , and M_5 are the same as in Case A, we obtain a similar result

$$M_4 U_4^1 + M_5 U_5^1 + M_4 (Y_4 - Y_5) = M_4 U_2^1 + M_5 U_1^1 .$$

Now, superimposing a speed $+U_0$ so that the bird and mitigator proceed to the right, equation (2B) becomes

$$(M_1 + M_3) U_0 = M \bar{V} = (M_1 + M_5) U_1 + (M_2 + M_4) U_2 \quad (3B)$$

Thus, the momentum equation (3B) is the same as that which would result by assuming that the entire crushed and uncrushed masses move at speeds U_2 and U_1 , respectively.

Again, since no external forces act on the system, time differentiation of equation (3B) gives

$$(M_1 + M_5) A_1 + (M_2 + M_4) A_2 + M_4 (\dot{U}_2 - \dot{U}_1) = 0 . \quad (4B)$$

The force transmitted to $(M_1 + M_5)$ at the crushed and uncrushed mitigator interface is produced solely by the dynamic crush force of the mitigator,

$$A_1 = -F / (M_1 + M_5) . \quad (5B)$$

Accordingly, this force (in the opposite direction) plus the force arising from the change in momentum per unit time of the mitigator occurring at the interface of the crushed and uncrushed masses, $M_4(U_1 - U_2)$, is the force acting on $(M_2 + M_4)$. Accordingly,

$$A_2 = (F + M_4(U_1 - U_2)) / (M_2 + M_4) . \quad (6B)$$

Case C: Mitigator Adjacent To MEM And Mitigator Crushes At MEM Face, and

Case D: Mitigator Moves With Bird And Mitigator Crushes At Bird Face.

In each case, stress wave effects cause undesirable, non-smooth, somewhat random pulse shape irregularities and some crush may occur at each end of the mitigator. Accordingly, these two cases are not considered practical for impact testing.

3.3 Energy Conservation

In both Cases A and B, energy is dissipated by deformation of the mitigator. In each case, the deformation energy amounts to

$$E_1 = \int F(U_1 - U_2) dt . \quad (7)$$

In addition, the system loses energy at the crush front (the interface separating the crushed and uncrushed masses) through collision between the crushed and uncrushed mitigator masses. Denoting the mass of a particle by M , the loss in kinetic energy produced by this type of impact amounts to

$$1/2 EM(U_1 - U_2)^2 ,$$

where U_1 and U_2 are the velocities before and after impact.² The impacts are inelastic, since the relative velocity between the involved masses is zero following impact. In our case, the progression of the crush front involves a continuous impact process so that the energy dissipated by this mechanism amounts to

$$W = 1/2 \int M \dot{A} (U_1 - U_2)^2 dt . \quad (8)$$

The total energy dissipated by the system is $E_1 + W$. Calculations show that the ratio $W/E_1 \approx 0$ for $U_0 = 100$ (where values of $U_1 - U_2 < 100$ ft/sec), and increases with increasing $(U_1 - U_2)$ to 0.05 when $U_0 = 500$ ft/sec.

²E. T. Whittaker, A Treatise on the Analytical Dynamics of Particles and Rigid Bodies, 4th ed., Dover Publications (1944), pp. 234-5.

Case A: The kinetic energy of the bird prior to impact is the energy of the system. The energy balance at any time during impact is given by

$$E_0 = E_1 + E_2 + W, \quad (9)$$

where E_1 and W are given by equations (7) and (8),

$$E_0 = M_1 U_0^2 / 2 \text{ and} \quad (10A)$$

$$E_2 = (M_1 + M_4) U_1^2 / 2 + (M_2 + M_5) U_2^2 / 2. \quad (11A)$$

Case B: The kinetic energy of the bird plus the mitigator prior to impact is the energy of the system. The energy balance at any time during impact is again given by equation (9) with E_1 and W given by equations (7) and (8), but where

$$E_0 = (M_1 + M_3) U_0^2 / 2 \text{ and} \quad (10B)$$

$$E_2 = (M_1 + M_5) U_1^2 / 2 + (M_2 + M_4) U_2^2 / 2. \quad (11B)$$

4. COMPUTER PROGRAMS

Programs were written for Cases A and B of section 3 for both mass and spring MEM's, giving rise to the impacts previously described. In each case, the motions of the bird, mitigator and MEM are completely determined by the momentum equations of section 3. The mitigator is shaped to produce a smooth pulse. The crush area of the shaped face increases linearly with the crush length from 0 to $4\pi \text{ in.}^2$ and thereafter remains constant and equal to $4\pi \text{ in.}^2$ *. The dynamic crush force is assumed to vary linearly with $(U_1 - U_2)$, and linear spring constants are assumed in the honeycomb and spring MEM.

*The crush area is slightly smaller than $4\pi \text{ in.}^2$ because the manufacture of honeycomb requires an opening of about 0.5 in. inside diameter.

4.1 VARYB

For Case B of section 3, the shaped face of the mitigator moving with the bird in the gun impacts a mass MEM (fig. 8a). At the beginning of the pulse fall, signified by the condition $U1=U2$, the program assumes elasticity in the honeycomb with springs at each end (fig. 8b). The spring constants are $Z1$ and $Z2$, which are determined by the input displacements $C1$ and $C2$ and the forces acting on $M1$ and $M2$ at the time $U1=U2$. No elasticity is assumed until the fall begins. The pulse ends when the forces acting on $M1$, $M2$, and $M3$ are simultaneously zero. $C1$ and $C2$ can be independently adjusted to provide agreement between the calculated and experimental pulse fall time.

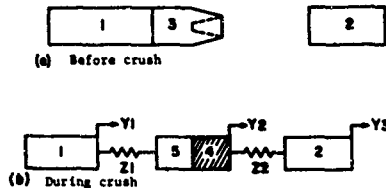


Figure 8. Notation for shaped mitigator attached to bird with a mass MEM.

With appropriate changes in the equations for $A1$ and $A2$, this program can be also run for Case A.

4.2 PULSE1

For Case B, the shaped mitigator moving with the bird impacts the spring MEM (fig. 9a). The spring in the MEM loads during the mitigator crush, so that the equations of motion take into account displacements of the forward and aft sections of the MEM as well as the displacements of the bird. Again, no honeycomb elasticity is assumed until the beginning of the pulse fall, which corresponds to the condition $U1=U6$.

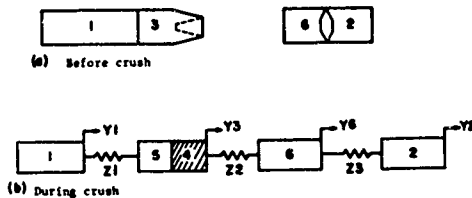


Figure 9. Notation for shaped mitigator attached to bird with spring MEM.

The fall is now governed by a 3-spring, 4-mass system (fig. 9b). The spring constants Z_1 , Z_2 are determined by input displacements C_1 , C_2 , and the forces acting on M_1 , M_2 at the time $U_1=U_6$; Z_3 is the value appropriate for the railroad springs in the MEM. The pulse terminates when the forces acting on M_1 , M_2 , M_3 , and M_6 are simultaneously zero. Again, C_1 and C_2 are adjusted to provide agreement between the calculated and experimental pulse fall time.

With the appropriate equations for A_1 and A_2 , this program can be run for Case A.

4.3 PULSE3

The equations and program describe the same impacts as PULSE1. In PULSE3, the experimental pulse fall $A_1(T)$ is assumed known together with $Z_1=Z_2$, since $R=0$. The $C_1=C_2$ are adjusted to provide agreement with the experimental pulse fall $A_1(T)$. Thus, PULSE1 and PULSE3 assume linear and nonlinear honeycomb elasticity, respectively. Hence, PULSE3 can be used to empirically determine the nonlinear elasticity of the mitigator.

4.4 JMEM and JBIRD

JMEM and JBIRD are abridged versions of VARYB and PULSE1 for the mitigator crushing at the MEM and bird interfaces, respectively. These programs are presented to show that the momentum and energy balances described in section 3 are satisfied, using the stated expressions for A_1 , A_2 , etc. JBIRD and JMEM do not take into account mitigator shaping. Moreover, for the above purpose, it was convenient to neglect the elasticity terms (which are point functions) and the programs terminate when $U_1=U_2$.

It is an easy matter to include the JMEM and JBIRD programs within VARYB or PULSE1. The conservation of momentum and energy could then be demonstrated in VARYB and PULSE1, with appropriate terms included for the springs. However, it was preferred not to further add to the printout of these programs.

5. THEORETICAL AND EXPERIMENTAL RESULTS

The impact of two solid bodies results in the production of compression waves at the impact surface. In a one-dimensional analysis, the waves propagate through each body at the elastic and/or plastic sound speed, reflect at the end surface, and propagate back toward the impact surface. The waves partially reflect and transmit at the impact surface, and the process repeats until the energy contained in the waves is dissipated. The strengths of the waves are a function of the impact force. For aluminum or steel impacting bodies, the wave speed through each body is approximately 200,000 in./sec, so that the wave system can produce substantial variations of the force acting at each section of each body in a typical pulse duration of 1 msec.

The data described in sections 5.1 through 5.4 and given in tables I through III and figures 10 through 15 refer to experiments made in the 4-in. gun at bird impact speeds of 400 to 500 ft/sec and mitigator static crush strengths of 8000 ± 800 psi. The results of additional tests, described in section 5.5 and given in figures 16 through 18, refer to bird impact speeds in the range 300 to 650 ft/sec and mitigator static crush strengths between 725 and 4000 psi.

As an example of the effect on the entire pulse caused by the system of shock waves arising from a high initial impact force, consider the acceleration-time history arising from the impact between a flat-faced aluminum honeycomb mitigator moving with the bird in the gun and a mass MEM, figure 10, shot number 1352.* The bird and mitigator were driven by atmospheric air through a vacuum and attained an impact speed of 470 ft/sec. The mitigator, bird, and MEM masses were 0.26, 1.38, and 24.4 kg and their lengths were 2.01 (original uncrushed mitigator length), 3.5, and 5 in. The bird was aluminum and the MEM was steel. The mitigator static crush force was $100,000 \pm 10,000$ lbs. As will be discussed later in this section, the dynamic crush force exceeds the static crush force and appears to be a smooth monotonic nondecreasing function of the bird speed relative to the MEM.

*All shots refer to tests made with the Harry Diamond Laboratories' 4- and 7-in. air guns.

TABLE IA. SUMMARY OF CALCULATED FORCES AND MOTIONS OF SYSTEM COMPONENTS
FOR CONICAL MITIGATOR ATTACHED TO BIRD, WITH SPRING MEM AND
LINEAR HONEYCOMB ELASTICITY

PULSE1 16:03EST 11/21/75

FB=J V1=J U0=7 121000.3.460

TIME	-A1	U1	Y1	A2	U2	Y2	A6	U6	Y6	F	R	F3
0.	.0	460.	.01	.0	.0	.00	.0	.0	.00	.0	.0	.0
102.	7.9	447.	.57	.1	.1	.00	8.0	14.2	.01	30.3	4.5	125
200.	14.6	410.	1.07	.9	1.6	.00	11.5	46.6	.04	55.1	6.0	107.3
300.	19.8	354.	1.53	2.5	7.8	.01	9.8	81.9	.12	73.6	4.6	297.3
400.	23.1	285.	1.92	4.5	16.3	.02	5.5	106.6	.23	84.6	2.4	557.3
500.	24.4	208.	2.21	6.3	35.7	.05	1.1	116.9	.37	88.8	.7	820.4
600.	24.9	128.	2.41	6.5	82.5	.13	.7	69.6	.46	89.9	.3	850.1
674.	24.4	71.	2.50	6.2	97.3	.21	1.0	71.6	.52	87.9	.0	807.7

SPRING CONSTANTS C1,C2=? .055.005

TIME	-A1	U1	X1	A2	U2	X2	A3	U3	X3	A6	U6
700.	24.4	49.	.055	6.0	103.	.000	130.9	106.	.295	*-12.1	62.
750.	9.0	23.	.020	5.4	112.	.005	*-102.0	37.	.271	2.7	63.
800.	13.6	4.	.031	4.8	120.	.000	77.5	38.	.239	-9.6	56.
850.	.0	-5.	.000	3.9	127.	.000	.0	84.	.194	-7.8	42.
900.	.0	-5.	.000	2.8	133.	.000	.0	-4.	.140	-5.7	39.
950.	.0	-5.	.000	1.6	136.	.000	.9	-4.	.081	-3.3	32.
1000.	.0	-5.	.000	.3	138.	.000	.0	-4.	.017	-.7	29.
1016.	.0	-5.	.000	.0	138.	.000	.0	-4.	.000	.0	00.

PULSE1 16:07EST 11/21/75

FB=J V1=J U0=7 122000.3.460

TIME	-A1	U1	Y1	A2	U2	Y2	A6	U6	Y6	F	R	F3
0.	.0	460.	.01	.0	.0	.00	.0	.0	.00	.0	.0	.0
102.	8.0	446.	.57	.1	.1	.00	8.1	14.3	.01	30.5	4.5	125
200.	14.7	410.	1.07	.9	1.6	.00	11.6	46.9	.04	55.6	6.0	107.3
300.	19.9	354.	1.53	2.5	7.8	.01	9.8	82.4	.12	74.1	4.6	297.3
400.	23.2	283.	1.92	4.5	16.4	.02	5.5	107.1	.24	85.0	2.3	557.3
500.	24.5	206.	2.21	6.3	35.9	.05	1.1	117.4	.37	89.2	.7	820.9
600.	24.9	126.	2.41	6.6	78.5	.13	.5	78.1	.47	90.0	.2	860.4
654.	24.5	55.	2.47	6.6	86.8	.18	.3	85.6	.52	88.4	.0	860.4

SPRING CONSTANTS C1,C2=? .06.005

TIME	-A1	U1	X1	A2	U2	X2	A3	U3	X3	A6	U6
700.	19.7	48.	.045	6.4	96.	.005	-42.0	149.	.324	.5	71.
750.	7.5	30.	.019	6.1	106.	.005	*-109.6	.0	.307	1.2	72.
800.	14.6	9.	.036	5.6	116.	.000	82.9	52.	.251	*-11.1	60.
850.	.0	-0.	.000	4.8	124.	.000	.0	104.	.240	-9.5	43.
900.	.0	-0.	.000	3.8	131.	.000	.0	-18.	.190	-7.5	40.
950.	.0	-0.	.000	2.6	136.	.000	.0	-18.	.130	-5.1	30.
1000.	.0	-0.	.000	1.3	139.	.000	.0	-18.	.064	-2.5	24.
1048.	.0	-0.	.000	.0	140.	.000	.0	-18.	.000	.0	00.

TABLE IA. SUMMARY OF CALCULATED FORCES AND MOTIONS OF SYSTEM COMPONENTS FOR CONICAL MITIGATOR ATTACHED TO BIRD, WITH SPRING MEM AND LINEAR HONEYCOMB ELASTICITY (Cont'd)

PULSE1 16:11EST 11/21/75

F0=: V1=: U0=? 121000.3.460

TIME	-A1	U1	Y1	A2	U2	Y2	A6	U6	Y6	F	R	F3
674.	24.4	71.	2.50	5.2	97.3	.21	1.0	71.6	.52	87.9	.0	80.7

SPRING CONSTANTS C1,C2=? .065,.001

TIME	-A1	U1	X1	A2	U2	X2	A3	U3	X3	A6	U6
700.	24.4	49.	.065	6.0	103.	.000	138.9	115.	.298	**12.1	61.
750.	10.6	22.	.028	5.4	112.	.001	-93.4	38.	.271	2.7	63.
800.	13.5	3.	.036	4.8	120.	.000	76.6	32.	.239	-9.6	57.
850.	.3	-8.	.000	3.9	127.	.000	.0	89.	.194	-7.9	43.
900.	.0	-8.	.000	2.9	133.	.000	.0	-4.	.142	-5.7	40.
950.	.0	-8.	.000	1.7	136.	.000	.0	-4.	.083	-3.4	33.
1000.	.0	-8.	.000	.4	138.	.000	.0	-4.	.019	-1.8	30.
1015.	.0	-8.	.000	.0	138.	.000	.0	-4.	.000	.0	30.

TABLE IB. SUMMARY OF CALCULATED FORCES AND MOTIONS OF SYSTEM COMPONENTS FOR CONICAL MITIGATOR ATTACHED TO BIRD, WITH SPRING MEM AND NONLINEAR HONEYCOMB ELASTICITY

PULSE3 11:48EST 11/21/75

F0=: V1=: U0=? 121000.3.460

TIME	-A1	U1	Y1	A2	U2	Y2	A6	U6	Y6	F	R	F3
674.	24.4	71.	2.50	6.2	97.3	.21	1.0	71.6	.52	87.9	.0	80.7

C1= J C2= J T3=? .06.06.00102

TIME	-A1	U1	X1	A2	U2	X2	A3	U3	X3	A6	U6
700.	20.4	50.	.057	6.0	103.	.000	-6.2	69.	.300	-1.3	71.
750.	12.7	24.	.043	5.6	112.	.054	-17.9	46.	.277	-3.2	68.
800.	5.5	10.	.032	4.9	121.	.036	-4.4	28.	.246	-6.8	59.
850.	3.8	3.	.020	4.1	128.	.020	.4	26.	.203	-6.3	48.
900.	3.1	-3.	.005	3.0	134.	.008	-11.0	21.	.151	-3.6	40.
950.	1.9	-6.	.000	1.9	138.	.000	.0	6.	.092	-3.7	34.
1000.	.8	-9.	.000	.6	139.	.000	.0	6.	.029	-1.2	30.
1024.	.0	-9.	.000	.0	140.	.000	.0	6.	.000	.0	30.

PULSE3 11:52EST 11/21/75

F0=: V1=: U0=? 121000.3.460

TIME	-A1	U1	Y1	A2	U2	Y2	A6	U6	Y6	F	R	F3
674.	24.4	71.	2.50	6.2	97.3	.21	1.0	71.6	.52	87.9	.0	80.7

C1= J C2= J T3=? .08.08.00102

TIME	-A1	U1	X1	A2	U2	X2	A3	U3	X3	A6	U6
700.	20.4	50.	.077	6.0	103.	.000	-4.7	70.	.300	-1.4	71.
750.	12.7	24.	.062	5.6	112.	.075	-16.2	50.	.277	-3.3	67.
800.	5.5	10.	.048	4.9	121.	.061	-8.3	29.	.245	-6.4	59.
850.	3.8	3.	.037	4.1	128.	.043	-3.5	21.	.203	-6.0	49.
900.	3.1	-3.	.026	3.0	134.	.027	-1.2	17.	.151	-4.5	40.
950.	1.9	-6.	.013	1.9	137.	.015	-1.6	16.	.092	-2.6	35.
1000.	.8	-9.	.001	.6	139.	.003	-3.8	8.	.029	-1.3	31.
1026.	.0	-9.	.000	.0	140.	.000	.0	7.	.000	.0	32.

TABLE IB. SUMMARY OF CALCULATED FORCES AND MOTIONS OF SYSTEM COMPONENTS FOR CONICAL MITIGATOR ATTACHED TO BIRD, WITH SPRING MEM AND NONLINEAR HONEYCOMB ELASTICITY (Cont'd)

PULSE3												
11:45EST 11/21/75												
F0=1 V1=1 U0=? 121000.3,460												
TIME	-A1	U1	Y1	A2	U2	Y2	A6	U6	Y6	F	R	F3
674.	24.4	71.	2.50	6.2	97.3	.21	1.0	71.6	.52	87.9	.0	80.7
C1=1 C2=1 T3=? .1, .1, .00102												
TIME	-A1	U1	X1	A2	U2	X2	A3	U3	X3	A6	U6	
700.	20.4	50.	.097	6.0	103.	.100	-3.8	70.	.300	-1.5	71.	
750.	12.7	24.	.081	5.6	112.	.096	-14.3	54.	.277	-3.5	67.	
800.	5.5	16.	.064	4.9	121.	.084	-9.6	33.	.245	-6.3	59.	
850.	3.8	3.	.052	4.1	128.	.068	-6.6	21.	.203	-5.7	49.	
900.	3.1	-3.	.042	3.0	134.	.051	-3.5	12.	.151	-4.3	41.	
950.	1.9	-6.	.033	1.9	137.	.035	-5	10.	.093	-2.7	35.	
1000.	.8	-9.	.023	.6	139.	.020	.5	10.	.030	-8	32.	
1050.	.0	-9.	.011	.0	140.	.007	.0	10.	.000	.0	32.	
1100.	.0	-9.	.000	.0	140.	.000	.0	10.	.000	.0	32.	
C1=1 C2=1 T3=?												

A smooth pulse can be obtained by reducing the strength of the wave system arising from the impact. To this end, we first note that the elastic and plastic wave speeds are at least an order of magnitude greater than the above bird speed and, because of energy dissipation, the strength of the waves diminishes as they traverse the body. Hence, the entire pulse can be made as smooth as desired by producing, in time, a continuous progression of sufficiently small strength impacts, each impact increasing the deceleration, until the desired bird deceleration is attained. Physically, this kind of impact force can be impressed on the bird by shaping the mitigator so that the mitigator crush area smoothly and continuously increases with the bird penetration over the period of the pulse rise. In addition, springs in the MEM are helpful in providing a continuously smooth increasing impact force with time.

For smooth pulses, the conservation equations of section 3 may be applied to the determination of the motions of the bird, mitigator, and MEM for the entire pulse. The following discussion is limited to a comparison of calculated and test results for shaped mitigators with both mass and spring MEM's.

5.1 Conical Shaped Mitigator on the Bird with a Mass MEM

Typical experimental data of bird deceleration with time are shown in figures 11a and 11b for shots 1703 and 1709, using the conical mitigator illustrated in figure 4. The mitigator altitude (shear section) and base (constant area section) lengths were 1.79 and 1.70 in., respectively. The experimental curves are fairly smooth, but exhibit times where the pulse abruptly changes slope; such changes typically occur on the passage of a shock or stress wave. Thus, in 1703 and 1709, stress waves produce changes in deceleration of about 4,000 g.

TABLE II. SUMMARY OF CALCULATED FORCES AND MOTIONS OF SYSTEM COMPONENTS FOR DOUBLE-WEDGE MITIGATOR ATTACHED TO BIRD, WITH SPRING MEM

FO=1 TIME	V1=1 -A1	U0=2 U1	Y1	A2	U2	Y2	A6	U5	Y6	F	R	F3
0.	.0	453.	.01	.0	.0	.00	.0	.0	.00	.0	.0	.0
102.	11.2	434.	.56	.2	.2	.00	12.2	21.0	.01	45.6	7.7	2.3
200.	19.9	304.	1.04	1.4	2.4	.00	15.6	63.4	.00	79.3	8.2	15.5
300.	25.2	312.	1.46	3.5	10.2	.01	11.1	112.5	.17	98.6	4.3	42.4
400.	26.9	225.	1.78	5.9	25.4	.03	4.4	137.2	.33	*174.0	1.0	76.7
500.	26.0	139.	2.00	6.6	80.6	.10	1.9	80.3	.44	99.4	.4	86.4
564.	24.8	89.	2.08	6.6	90.3	.17	1.2	89.9	.50	94.6	.0	86.4

TABLE III. SUMMARY OF CALCULATED FORCES AND MOTIONS OF SYSTEM COMPONENTS FOR DOUBLE-WEDGE MITIGATOR ATTACHED TO MEM, WITH SPRING MEM

FO=1 TIME	V1=1 -A1	U0=2 U1	Y1	A2	U2	Y2	A6	U6	Y6	F	R	F3
0.	.0	464.	.01	.0	.0	.00	.0	.0	.00	.0	.0	.0
102.	20.3	442.	.57	.1	.1	.00	8.8	15.3	.01	41.9	8.4	1.6
200.	23.6	389.	1.06	1.0	1.7	.00	13.1	51.7	.05	73.4	9.6	11.3
300.	23.6	317.	1.48	2.8	7.7	.01	11.4	92.5	.13	92.7	5.7	32.6
400.	23.3	240.	1.82	5.0	20.2	.02	5.8	121.0	.26	97.0	1.8	62.4
500.	21.6	163.	2.06	6.6	70.6	.07	.7	70.2	.40	91.0	1.2	86.4
600.	19.9	101.	2.22	6.6	85.4	.16	-.1	83.2	.49	85.5	.0	86.4
632.	19.5	82.	2.25	6.5	91.7	.19	-.3	83.0	.52	83.9	.0	85.9

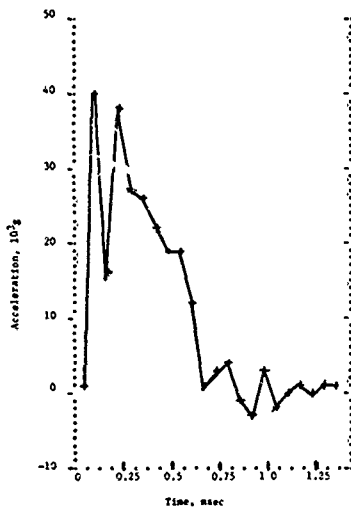


Figure 10. Setback acceleration for flat-faced mitigator attached to bird with mass MEM. M1=1380, M2=24400, M3=260, and U0=468. Shot 1352.

The static crush loading for the aluminum honeycomb in the above shots was experimentally determined as 90,000 ± 9000 lbs. The experimental data accumulated for setback deceleration show that the dynamic crush loading F is strain-rate sensitive and is given approximately by the relation

$$F = F_0 \frac{A}{(12.56)} [1 + V_1(U_1/U_0)]. \quad (12)$$

Here, $A \leq 12.56 \text{ in.}^2$ is the instantaneous crush area (the mitigators were shaped so that the crush area increased linearly with the bird penetration distance), and F_0 and V_1 are constants to be determined from the experimental data. As will be shown, the calculations can usually be brought into agreement with the test data for F_0 approximately 5 to 20 percent larger than the static crush strength and V_1 in the range 0.5 to 0.3 for $(U_1 - U_2) < 500 \text{ ft./sec.}$ The calculated curves were determined by using the computer program VARVB of section 4; (F_0, V_1) pairs were selected to provide agreement with the experimental data.

Specifically, agreement with experiment was sought for $A_1(T)$. There is some elasticity in the mitigator, and for this reason the time at which the mitigator crush ends (that is, when $U_1=U_2$) cannot be precisely determined from the experimental values of U_1 or A_1 . However, since momentum is conserved (eq (3A) and (3B)), the value of $U_1=U_2$ is independent of F_0 and V_1 . Thus, U_1 at the end of the crush is known. Except for a possible error of less than 30 μ sec in determining the beginning of the pulse, the experimental $U_1(T)$ is also well known. Hence, T at the end of the crush is also well defined. The crush time markedly decreases with increasing F . Hence, (F_0, V_1) pairs are selected in program VARYB to provide $A_1(T)$ agreement with experiment consistent with the above determined crush time. Although a unique (F_0, V_1) pair is not obtained, good agreement with experiment is limited to (F_0, V_1) pairs over small ranges of F_0 and V_1 .

The fall part of the pulse begins when $U_1=U_2$ and ends when $A_1=0$. The time duration and shape of the $A_1(T)$ pulse fall depends on the elasticity of the uncrushed part of the mitigator and is independent of (F_0, V_1) .

The possible strain under load of the bird and MEM is too small to account for the long time duration of the pulse fall. Hence, the pulse fall can only be explained by elasticity of the mitigator. Accordingly, we assume equal springs at each end of the mitigator and vary the values of the spring constant to obtain agreement with the experiment. The experimental data of the pulse fall are not sufficient to more than grossly define the elasticity of the honeycomb. In the calculations, using program VARYB, the spring constants are assumed to vary linearly with strain (strain-rate dependence was neglected) and values were selected to provide the appropriate time duration of the fall pulse.

In figure 11a, shot 1703, the calculated $U_1=U_2=31$ fps and the corresponding crush time obtained from the experimental $U_1(T)$ is 780 μ sec. Good agreement of $A_1(T)$ with experiment for the required crush time is obtained for $(F_0, V_1) = (80,000, 0.5)$.

To indicate the extent to which the dynamic crush force varies with the rate-of-strain, the required crush time is shown in figure 11a for $(100,000, 0)$. In this case, the calculated A_1 are much smaller than those of the experiment of the beginning and too large toward the end of the crush. In particular, the crush area is constant and the experimental $dA_1/dt < 0$ for $T > 440$. The calculated A_1 can only decrease with decreasing dynamic crush force.

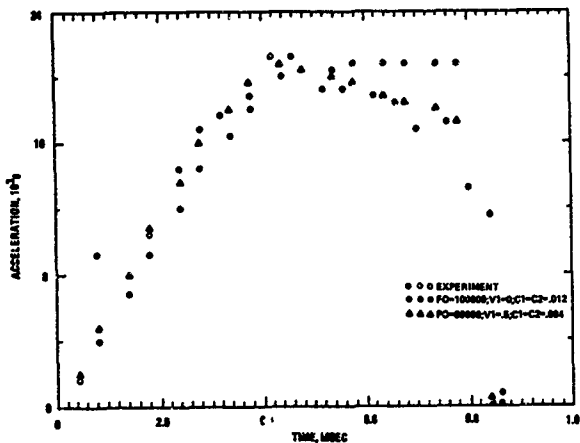


Figure 11a. Comparison of experimental and calculated setback acceleration for conical mitigator attached to bird with mass MEM. $M_1=2070$, $M_2=29,400$, $M_3=320$, and $U_0=412$. Shot 1703.

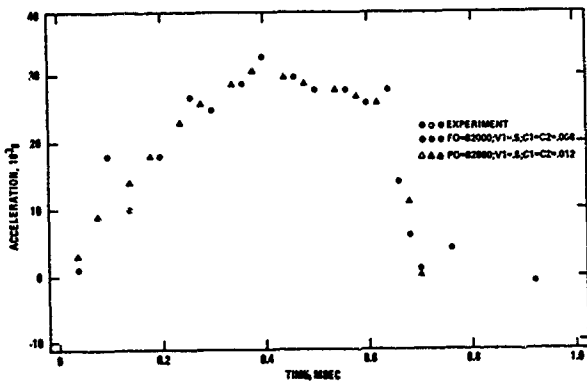


Figure 11b. Comparison of experimental and calculated setback acceleration for conical mitigator attached to bird with mass MEM. $M_1=1360$, $M_2=20,400$, $M_3=320$, and $U_0=483$. Shot 1799.

With reference to the change in crush time with F_0 and V_1 , calculations show that $-dF_0/dT = \text{constant} = +170 \text{ lb}/\mu\text{sec}$ in the range $75,000 < F_0 < 95,000 \text{ lb}$ and $-dV_1/dT = 0.0045/\mu\text{sec}$ for $0.4 < V_1 < 0.5$. For precision in determining the crush time to within $10 \mu\text{sec}$, F_0 is determined to within 2000 lb and V_1 is determined to within 0.05 .

Stress wave effects giving rise to abrupt changes in A_1 are apparent at times $80, 420, \text{ and } 460 \mu\text{sec}$. However, since the velocity at the end of the crush is independent of F , and since the experimental $U_1(T)$ is, in effect, a time-wise integration of A_1 , the crush time is little affected by stress waves of short duration. The calculated data do not include stress wave effects; otherwise the $A_1(T)$ agreement with experiment is within about 10 percent.

The experiment shows $A_1=0$ at $T=850 (+0 \text{ and } -25) \mu\text{sec}$. The calculations give $A_1=0$ at 834 and $856 \mu\text{sec}$ for $C_1=C_2=0.004$ and 0.008 in. , respectively.

Similarly, experimental and calculated data are shown in figure 11b for shot 1709. The calculated $U_1=U_2=36 \text{ ft}/\text{sec}$ and the corresponding crush time obtained from the experimental $U_1(T)$ is $630 \mu\text{sec}$. The required crush time is obtained for $(F_0, V_1)=(82,000, 0.5)$. Here, $dF_0/dT = \text{constant} = 220 \text{ lb}/\mu\text{sec}$ for $V_1=0.5$ in the range $80,000 < F_0 < 90,000 \text{ lb}$.

The experiment shows that $A_1=0$ at $T=700 \mu\text{sec}$ and then A_1 abruptly rises and falls to zero. The abrupt rise is probably caused by a stress wave, and will be discounted. The fall pulse was calculated for the two cases, $C_1=C_2=0.008$ and 0.012 ; the resulting total pulse times are 692 and $706 \mu\text{sec}$.

5.2 Conical Shaped Mitigator on the Bird with the Spring MEM

In the case of the spring MEM, the end of the mitigator crush occurs at the instant $U_1=U_6$. Define U_C as the velocity marking the end of the crush. For given values of the system masses, U_0 , and if $U_1=U_2=U_6=U_C$, momentum conservation yields a unique value for U_C that is independent of F and F_3 . Then, as in the previous section, the time duration of the mitigator crush, T_C , is determined from the experimental $U_1(T)$. With this value for T_C , we can proceed to select a set of (F_0, V_1) pairs and corresponding calculated data to fit the experimental $A_1(T)$.

However, for the spring MEM, depending on (F_0, V_1) and F_3 , it is possible for $U_2 > U_6$ at the instant $U_1=U_6$. Accordingly, U_C is not uniquely determined from momentum conservation. Furthermore, because of elasticity in the honeycomb and MEM, there is no marked reduction of A_1

at $T=TC$, and consequently, TC cannot be precisely determined from the experimental $A_1(T)$. Nevertheless, for TC obtained from the condition $U_1=U_2=U_6=UC$, calculations showed that small variations of (F_0, V_1) had little effect on A_1 and U_1 for all $T < TC$, whether or not $U_2=U_6$ at $T=U_6$. Consequently, in our procedure, TC was found for a (F_0, V_1) pair yielding $U_1=U_2=U_6=UC$; then, for the same TC , (F_0, V_1) pairs were selected for use in the calculations so as to fit the experimental A_1 for $0 < T < TC$. All calculations were made using the programs PULSE1 and PULSE3 (sects. 4.2 and 4.3), which assume linear and nonlinear honeycomb elasticity, respectively. As was the case for the mass MEM, the beginning of the crush of the mitigator can usually be determined to within 30 μsec .

A series of tests for evaluating fuze components were run in the HDL 4-in. gun, all with $U_0=460 \pm 2$, $M_1=1480$, $M_3=260$, the spring MEM of section 2, and the conical mitigator shown in figure 4. Here, the measured static crush was $107,000 \pm 10,000$ lb. The crush area, A , varied linearly with the bird penetration (Y_1-Y_6) in the manner

$$A = 12.56 (Y_1 - Y_6) / 2.85 \text{ for } 0 < Y_1 - Y_6 < 2.85 \text{ and}$$

$$A = 12.56 \quad \text{for } Y_1 - Y_6 > 2.85$$

For the given test conditions, the calculated bird penetration $(Y_1 - Y_6)$ was less than 2.85 in. The measurement error in the determination of A_1 is random and amounts to 400 g for film readings of the bird displacement at 50 μsec intervals. The measurement error changes approximately as the inverse square of the film reading time interval. The measurement error is 400 g for the given data, except that the error is 200 g for the data given in figure 16b.

The experimental $A_1(T)$ for the seven tests are shown in figures 12a and 13a where each test is identified by the prefixed letter E. The scatter of the experimental A_1 is generally within $\pm 10^3$ g. Some of the scatter arises from stress waves, which can be seen from the data as sudden changes in dA_1/dT . Some scatter also arises from measurement error and the error in determining the beginning of the crush. For some mitigator shapes with large altitudes, and also depending on the honeycomb crush strength, the crush does not completely occur in a column-like manner. In this case, the resulting dynamic crush strength is somewhat less than expected for the given cross-sectional area.

Momentum conservation gave $U_1=U_2=U_6=UC=85$ ft/sec and, following the above procedure, the $U_1(T)$ from the seven tests gave $TC=665 \pm 10$ μsec . This suggests that the error in determining the beginning of the crush for the above tests was closer to ± 10 μsec . In

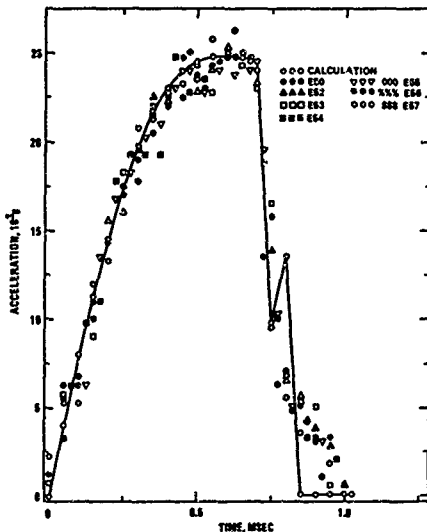


Figure 12a. Comparison of experimental and calculated setback acceleration of 7 shots for conical mitigator attached to bird with spring MEM. Shots 1850; 1852-1857, M1=1480, M3=260, U0=460, and TC=665.

addition, it is interesting to observe that the experimental velocity at the end of the pulse for the seven tests was -6 ± 2 ft/sec. Apparently, the experiments are repeatable with a high degree of precision; generally, A1 is repeatable to within ± 5 percent.

The calculated A1(T) for TC of 665 and 683 and various (F0,V1) are given in figures 12b and 13b, respectively. For each TC, the agreement between the calculations of each set is ± 1000 g, except toward the end of the pulse where the spread increases to 5000 g. Comparing the two sets of calculations at V1 of 0.7, 0.5, and 0, the maximum difference in A1 at any TC=665 amounts to 1000 g. The calculations for V1 of 0.3 and 0.2 are also shown in figures 12a and 13a, respectively. Excluding the fall part of the pulse, agreement with the experimental data is about ± 1000 g. For TC=665, good fit with the experimental data is obtained for the (F0, V1) range (117,000, 0.2) to (102,000, 0.5). Once again, as can be seen from the curve for V1=0, the dynamic crush force is a function of (U1-U6) and is significantly larger than the static crush force.

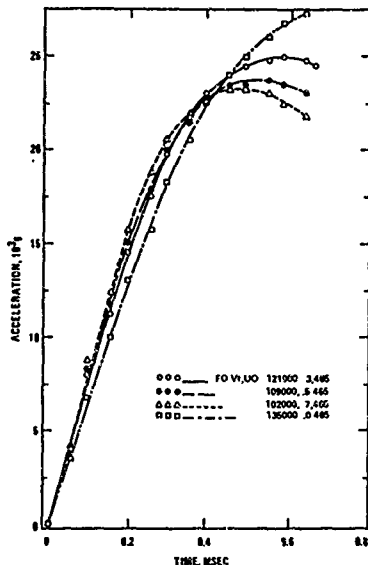


Figure 12b. Calculated setback acceleration for conical mitigator attached to bird with spring MEM for various dynamic crush strengths. TC=665.

Assuming linear honeycomb elasticity, program PULSE1 calculations for the fall part of the pulse are shown in figures 12a and 13a for $C1=0.06$ and $C2=0.01$, where $C1$ and $C2$ are the displacements of the honeycomb at the bird and MEM ends, respectively, arising from relaxing the loads thereon occurring at $T=TC$. Hence, the selection of $C1$ and $C2$ and the forces acting at each end of the honeycomb determine the spring constants for the honeycomb; their values were chosen so that the calculations would provide

- (1) the experimental terminal $U1$, and
- (2) the experimental pulse fall time.

Calculations showed that the experimental terminal $U1 = -6 \pm 2$ ft/sec would be obtained for some values of $C1$, $C2$ when $C1 + C2 = 0.065 \pm 0.01$. However, in order to avoid large oscillations of $A1$, which do not appear in this experimental data, calculations show

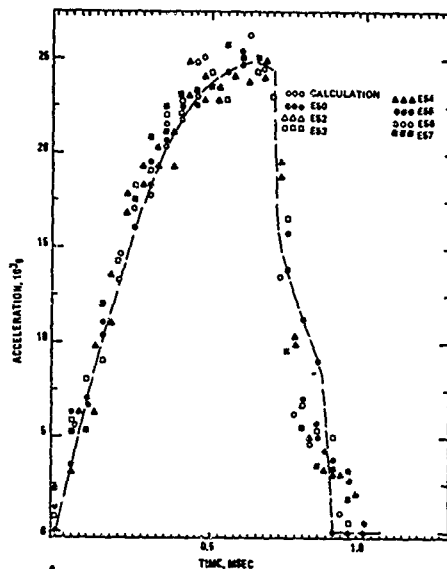


Figure 13a. Comparison of experimental and calculated setback acceleration of 7 shots for conical mitigator attached to bird with spring MEM. Shots 1850; 1852-1857, M1=1480, M3=260, U0=460, and TC=688.

that $C1 \gg C2$. For the above $C1$ and $C2$ limits, the calculated $A1$ largely exceeded those of the experiments in the neighborhood of $T > TC$. Consequently, the matching of the experimental $U1$ resulted in calculated pulse fall times that were always too small (figs. 12a and 13a).

Apparently, the model of three linear springs is not correct, and allowance for elasticity involving the equivalent of some nonlinearity in the springs is required to provide an adequate pulse fall. In particular, the $A1$ response is very sensitive to the honeycomb elasticity.

Table IA is a summary of a typical calculation of the forces acting on and the motion of the various components of the system for $(F0, V1) = (121,000, 0.3)$ and $(122,000, 0.3)$ for several values of $C1, C2$.* The accelerations $A1, A2, A6$ are given in units of $10^3 g$ and the forces $F, R, F3$ are in units of $10^3 lb$. The bird penetration of the

*In the calculations, $TC = 665$ at $(F0, V1) = (121,150, 0.3)$.

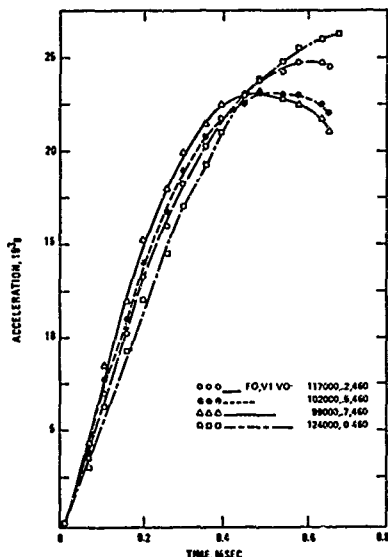


Figure 13b. Calculated setback acceleration for conical mitigator attached to bird with spring MEM for various dynamic crush strengths. TC=688.

honeycomb, (Y1-Y6), amounts to 2.0 in., at which point the crush force is 88,000 lb. For each FO, the maximum spring MEM loading of 86,400 lb is reached between 500 and 600 usec. It is interesting to note that the hydrodynamic force $R=M4(U1-U6)$ arising from the honeycomb crush amounts to 15 percent of F at 100 usec. Thereafter, R/F falls rapidly, since R varies as $(U1-U6)^2$. Although TC differs by 20 usec for the two values of FO, the change of Al(T) is negligible. Of course, because of the same UC, the difference in Al(T) between the two pulse falls is accounted for by this 20 usec difference. For each C1, C2, we observe a rapid fall of Al(T) with oscillation.

In PULSE3, $Z1=Z2=-A1*M1/X1$ and $A3=Z1*(X1-X2)/M3$, where A1 is the experimental Al(T) and X1, X2 are the calculated instantaneous honeycomb elongations arising from the instantaneous force at each end of the honeycomb at $T \geq TC$. In this way, the honeycomb elasticity is made nonlinear. The spring MEM elasticity is linear and is the same as in PULSE1. In PULSE3, the displacements $X1=X2=C1=C2$ at $T=TC$ are selected input to provide the same pulse fall time as that of the experiment.

Using PULSE3, the calculated results for $(F0,V1)=(121,000, 0.3)$ and several values of $C1=C2$ are shown in table IB. Clearly, the time required for $X3$ to go to zero is essentially independent of the selected $C1, C2$. Moreover, $X3=0$, at the same time the experimental $A1=0$. Hence, the spring MEM determines the time duration of the pulse fall. Finally, $C1=C2$ are uniquely determined by the condition that simultaneously $X1=X2=X3=A1=0$ at the end of the fall.

For the values shown in table IB, the fall time increases with increasing $C1=C2$. For the total pulse time of 1.02 msec, to within 10 percent, $C1=C2=0.08$ is the required honeycomb elongation at $T=TC=674$ msec. Excluding the neighborhood $A1>0$ where the procedure is doubtful, $Z1=Z2$ is largest near $T=TC$ and decreases with increasing T by a factor of about 3.

Excluding the fall part of the pulse, the present calculations agree with those of the previous section for the mass MEM, where for the measured static crush of $90,000 \pm 9000$ lb, a good fit was found for $(F0,V1) = (80,000, 0.5)$. However, the shape of the present mitigator differs from that used for the mass MEM, and this can result in a change of $V1$ in characterizing the dynamic crush strength.

5.3 Wedge Mitigator on the Bird with a Spring MEM

Two tests were run in the HDL 4-in. gun at $U0=453$ with $M1=1630$, $M3=230$, the spring MEM of section 2, and the double wedge mitigator shown in figure 5. The altitude and base lengths were 1.5 and 0.9 in., respectively. The crush area varied approximately linearly with the bird penetration $(Y1-Y6)$, so that

$$A = 12.56(Y1-Y6)/1.5 \text{ for } Y1-Y6 < 1.5 \text{ and}$$

$$A = 12.56 \quad \text{for } Y1-Y6 \geq 1.5 .$$

Momentum conservation gave $UC=90$ and the TC from the experimental $U1(T)$ were found as 550 and 580 μsec for shot numbers 1897 and 1898. The experimental terminal velocities differ by only 2 ft/sec. Again, like those for the conical shaped mitigator, the present experiments appear to be very repeatable and the beginning of the crush can be determined to within 30 μsec .

The calculated $A1(T)$ for $TC=564$ with $(F0,V1) = (86,000, 0.5)$ is shown in figure 14 for $T \leq TC$. The scatter of the experimental data as well as the fit with the calculations is generally within ± 1000 g. The details of the forces acting on and the motions of the various components are summarized in table II. The bird penetration $(Y1-Y6)$ slightly exceeds the 1.5-in. altitude length of the wedge.

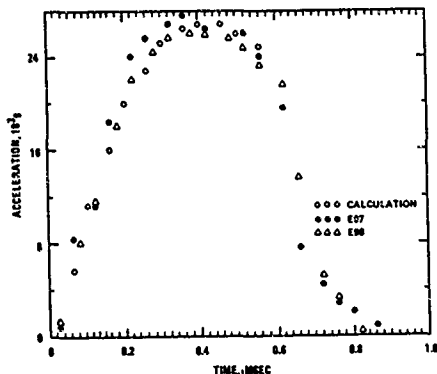


Figure 14. Comparison of experimental and calculated setback acceleration for double wedge mitigator attached to bird with spring MEM. M1=1630, M3=230, U0=453, and TC=564. Shots 1897 and 1898.

The pulse falls of the two tests are in close agreement, but no attempt was made to calculate the pulse falls or determine the spring constants. The slightly higher experimental terminal velocity found for tests 1897 and 1898, 5 ± 1 ft/sec, compared with those of the previous section (-6 ± 2 ft/sec), is due in part to the slightly higher efficiency of the gun at higher values of (M1+M3), (which results in higher projectile energy and a higher value for UC) and may also be due to a very small difference of honeycomb elasticity between the two mitigators.

Similar agreement (not presented here) in experimental scatter and between experimental and calculated data is found for the triple-wedge. The A1(T) for the two types of wedges are also in good agreement.

5.4 Mitigator Placed Adjacent to Spring MEM

It is preferable to place the mitigator adjacent to the MEM, rather than accelerate it in a gun, since the entire gun energy can then be used to drive the bird and payload. For a given maximum setback deceleration, this leads to an increase of U0 and a longer pulse time. Again, to avoid strong stress waves and obtain a smooth pulse, the mitigator crush must begin at the shaped face. For this reason the shaped face is turned around so that now the crush proceeds from the bird face toward the MEM. As noted in section 3, this affects the forces acting on M1 and M6.

The double-wedge mitigator described in the previous section, figure 5, with an altitude of 1.5 in. and a base length of 0.9 in., was placed with its base adjacent to the spring MEM. In this test, HDL shot number 1901, U0=464, M1=1800, and M3=210.

Momentum conservation gave UC=88 ft/sec and TC from the experimental U1(T) was found to be 600 μ sec. Again, the time of the beginning of the crush is known only to within about 30 μ sec, so that calculations were made for TC of 598 and 632 μ sec at (F0,V1) of (82,000, 0.5) and (77,000, 0.5), respectively. To form a common basis of comparison, 30 μ sec was subtracted from the plot of the latter calculations. As shown in figure 15, the agreement between the calculated and experimental data is generally to within 2000 g for TC=598 μ sec and about 1000 g for TC=632 μ sec. The details of the forces acting on and the motions of the various components are summarized in table III for TC=632.

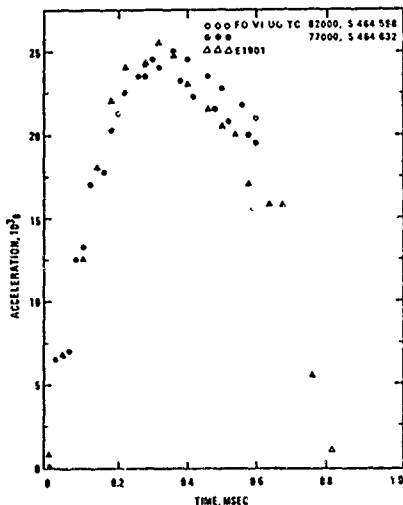


Figure 15. Comparison of experimental and calculated setback acceleration for double-wedge mitigator attached to spring MEM. M1=1800, M3=210, U0=464, TC=598, and TC=632. Shot 1901.

5.5 Additional Data

Additional tests were performed with double-wedge mitigators for static crush strengths of 725, 2130, and 4350 psi at bird impact speeds between 300 and 650 ft/sec. The results of these tests and calculations based on the conservation equations are given in figures 16, 17, and 18.

Figure 16a shows 7-in. gun test data and the results of calculations using VARYB for $U_0=648$, $P=725$, and with the mitigator attached to a mass MEM. Test data were not recorded for $T>0.7$ msec, so that part of the pulse during the mitigator crush and the entire pulse fall is missing. Figure 16b gives 4-in. gun test data and the results of calculations using VARYB for $U_0=318$, $P=725$, and with the mitigator again attached to a mass MEM. For each test, the difference of $A_1(T)$ between experiment and calculation for $(F_0, V_1) = (1.2P, 0.3)$ is well within 10 percent of $A_1(T)$. The fall pulse shown in figure 16b arises entirely from the elasticity in the uncrushed honeycomb. As noted in section 5.1 and in the present calculation, a good fit with the test data is obtained for $C_1=C_2=0.01$. Here, the pulse fall amounts to about 350 μ sec, compared with the 100 μ sec fall obtained in section 5.1. The reason for the longer fall arises from the larger values of M_1 and M_2 and smaller A_1 at the time $U_1=U_2=U_C$.

The shot of figure 16b was designed to obtain a nearly constant pulse of long duration by controlling the mitigator area. Accordingly, the double-wedge altitude amounted to 2 in., and the mitigator cross-sectional area linearly increased in this length from 0 to only 7.8 in.² This area then further increased linearly to 12.56 in.² in a length of 16 in. The experimental bird penetration, δ , amounted to 17.5 in. and the predicted value was 17.8 in. Generally, the difference between calculated and test values of δ for either bird or MEM penetration of the mitigator is within about 4 percent of δ .

Calculated and test data $A_1(T)$ for $450 < U_0 < 500$ with P of 2130 and 4350 and the mitigator attached to the MEM are shown in figures 17 and 18, respectively. A better fit with the test data, especially the slope dA_1/dT from the maximum value of A_1 to A_1 at $T=TC$ is given by $(F_0, V_1) = (1.05P, 0.5)$ than for $(1.2P, 0.3)$. Again, for each set of calculations, the difference between the calculated and test data $A_1(T)$ is within 10 percent of $A_1(T)$.

Apparently, the dynamic force (eq 12) adequately describes the crushing of honeycomb of various strengths in the range $725 < P < 8000$ psi at crush speeds up to at least 650 ft/sec. In agreement with the physical observation of the crushes, this means that honeycomb crush occurs in approximately the same manner over the above ranges of P and crush speed.

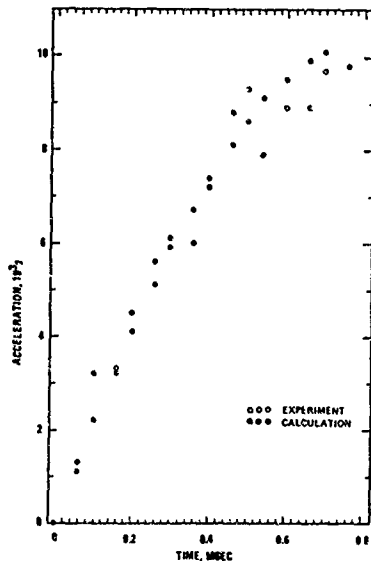


Figure 16a. Comparison of experimental and calculated setback acceleration in the 7-in. gun for double-wedge honeycomb mitigator attached to mass MEM. Wedge altitude = 5 in., $P=725$, $M1=2530$, $M2=31280$, $M3=2160$, $U0=648$, and $(FO,V1) = (1.2 P, 0.3)$. Shot 53. (Data not available for $T>0.7$ msec.)

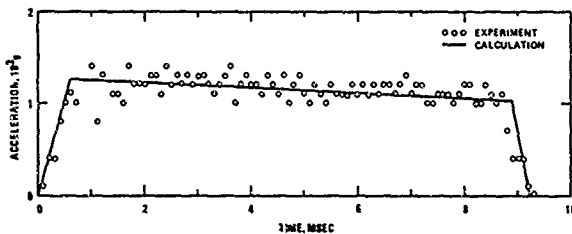


Figure 16b. Comparison of experimental and calculated setback acceleration for double-wedge honeycomb mitigator attached to infinite mass MEM. Wedge altitude = 2 in., $P=725$, $M1=4180$, $M3=1220$, $U0=318$, $C1=C2=0.01$ and $(FO,V1)=(1.2 F, 0.3)$. Shot 1984.

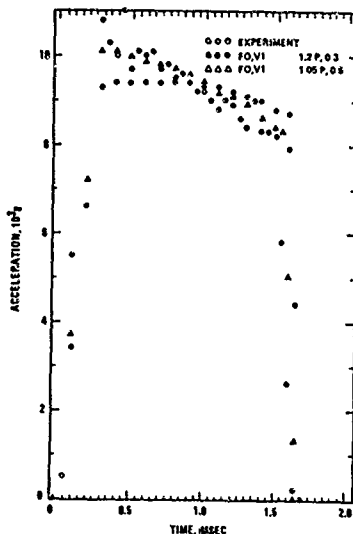


Figure 17. Comparison of experimental and calculated setback acceleration for double-wedge honeycomb mitigator attached to bird with mass MEM. Wedge altitude = 1.5 in., $P=2130$, $M_1=1580$, $M_2=30430$, $M_3=320$, $U_0=454$, and $C_1=C_2=0.01$. Shot 2022.

6. SUMMARY AND CONCLUSIONS

The use of variously shaped and various strength aluminum honeycomb mitigators together with stock-item railroad springs in the MEM has demonstrated that it is possible to obtain smooth, predictable, highly repeatable setback acceleration-time pulses for testing projectiles and/or components contained therein. The experimental scatter from test-to-test is found to be 1000 g for accelerations attaining a maximum of 25,000 g. The difference between experimental and theoretical setback accelerations based on the mass, momentum, and energy conservation equations is less than 10 percent for the rise and steady parts of the pulse. The crush can usually be predicted to within 4 percent of the bird or MEM penetration of the mitigator. The fall pulse is governed by the nonlinear system elasticity and the physical constants thereof are determined from experimental data.

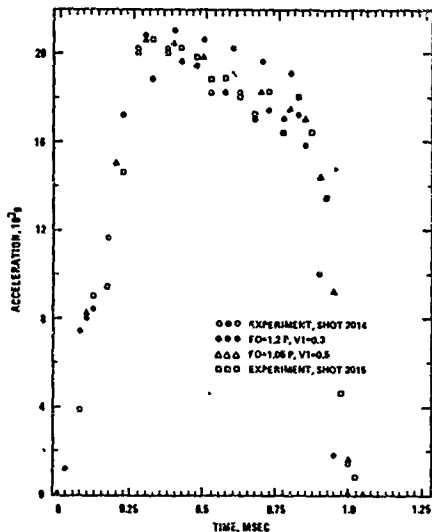


Figure 18. Comparison of experimental and calculated setback acceleration for double-wedge honeycomb mitigator attached to bird with spring MEM. Wedge altitude = 1.5 in., $P=4350$, $M1=1250$, $M3=300$, $U0=480$, $C1=0.06$, and $C2=0.01$. Shots 2014 and 2015.

The dynamic force equation (12) is derived from the experimental data and is of the same form for mitigator strengths of 725 to 8000 psi and crush speeds up to at least 650 ft./sec. The difference between experimental and calculated setback accelerations is within 10 percent for either (FO,V1) pairs (1.05P, 0.5) or (1.2P, 0.3). Pulse shapes may be varied over a wide range of rise and steady times, peak acceleration, etc., by varying the mitigator shape (crush area as a function of crush length), crush strength, projectile mass and spring MEM elasticity.

The spring MEM stores energy during the crush of the mitigator and, together with some small energy provided by elasticity of the mitigator, releases this energy at the termination of the crush. For an energy corresponding to a linear spring loading of 86,400 lb at a deflection of 0.331 in., the spring MEM provides a smooth pulse fall of about 300 μ sec for a 3.8 lb projectile attaining a peak setback deceleration of 25,000 g. This compares to a sharp pulse fall of about 100 μ sec for a mass MEM, where the elasticity is derived solely from the uncrushed mitigator.

7. LIST OF SYMBOLS

- A mitigator crush area at the bird or MEM interface, in.²
- AI acceleration, ft/sec²
- C1 honeycomb elongation at the bird interface, arising from relaxing the force thereon at T=TC, in.
- C2 honeycomb elongation at the MEM interface, arising from relaxing the force thereon at T=TC, in.
- C3 displacement of the spring in the spring MEM at T=TC, in.
- E0 either the initial kinetic energy of the bird (mitigator attached to MEM), or initial kinetic energy of the bird plus mitigator (mitigator attached to bird), ft-lb
- E1 energy dissipated by mitigator deformation, ft-lb
- E2 instantaneous kinetic energy of the system, ft-lb
- F mitigator dynamic crush force, lb
- F0 product of dynamic crush coefficient and P, used to determine mitigator dynamic crush force, equation (12), lb
- F3 force exerted by the spring in the spring MEM, lb
- I=1 bird
- I=2 mass MEM or aft section of spring MEM
- I=3 original uncrushed mitigator
- I=4 crushed mitigator
- I=5 remaining uncrushed mitigator
- I=6 forward section of spring MEM
- ℓ distance of mitigator crush front travel, in.
- (ℓ-δ) length occupied by crushed mitigator, in.
- L original mitigator length, in.

LIST OF SYMBOLS (Cont'd)

- M0 mass of railroad spring, g
- MI mass, g
- \dot{M}_4 ($=\rho AS(U1-U6)$ for spring MEM; $=\rho AS(U1-U2)$ for mass MEM), time rate of mitigator crush, lbm/sec
- P mitigator static crush pressure, psi
- R ($=\dot{M}_4(U1-U6)$ for spring MEM; $=\dot{M}_4(U1-U2)$ for mass MEM), hydrodynamic crush force, lb
- S ($=L/\delta$), ratio of crush front travel to depth of bird or MEM penetration
- T time, sec
- TC time duration of the mitigator crush, sec
- UC velocity at the termination of the mitigator crush, ft/sec
- UI velocity, ft/sec
- UO initial bird velocity, ft/sec
- V1 constant used in determining mitigator dynamic crush strength, equation (12), nondimensional
- W energy dissipated through collision between crushed and uncrushed mitigator masses, ft-lb
- YI displacement, in.
- δ depth of bird or MEM penetration, in.
- ρ density of uncrushed mitigator, lbm/in.³
- $\rho 1$ density of crushed mitigator, lbm/in.³

LIST OF SYMBOLS (Cont'd)

For Mass MEM

$X1=C1-Y3+Y1 \geq 0$, honeycomb elongation at bird interface, in.

$X2=C2-Y2+Y3 \geq 0$, honeycomb elongation at MEM interface, in.

$Z1(=-A1M1/C1)$, honeycomb spring constant at bird interface, where $A1$ is the acceleration at $T=TC$, lb/in.

$Z2(=-A1M1/C2)$, honeycomb spring constant at MEM interface, where $A1$ is the acceleration at $T=TC$, lb/in.

For Spring MEM

$X1=C1-Y3+Y1 \geq 0$, honeycomb elongation at bird interface, in.

$X2=C2-Y6+Y3 \geq 0$, honeycomb elongation at MEM interface, in.

$=C3-Y2+Y6 \geq 0$, spring displacement of spring MEM, in.

$Z1(=-A1M1/C1$, linear case; $=-A1M1/X1$, nonlinear case), honeycomb spring constant at bird interface where $A1$ is the acceleration at $T=TC$, lb/in.

$Z2(=-A1M1/C2$, linear case; $=-A1M1/X1$, nonlinear case), honeycomb spring constant at MEM interface, where $A1$ is the acceleration at $T=TC$, lb/in.

$Z3(=86,400/0.3308)$, spring constant for spring MEM, lb/in.

Superscript

(\cdot) denotes time differentiation of the given variable

6. CODES

8.1 VARYB 09/04/75
VARYB 14:15EDT

```
80 REK J=
90 PRINT "SHOT NUMBER IS":J
95 REK MIT AT REM * J=0
95 REK MIT AT BIRD, J<>0
100 G1=454*32.2
110 S=32000
120 K=1000
130 T1=2E-6
150 A1=1650/G1
160 X2=25200/G1
170 X3=i.195*64/1728
190 A0=12.56
200 S=1.3
210 D=1.105
240 PRINT "FO=: V1=: U0=: L=: J=:":
250 INPUT FO,V1,U0,L,J
260 U1=U0
270 *****
280 *****
290 PRINT " TIME -A1 U1 Y1 A2 U2 Y2 F H"
320 V=(U1-U2)/U0
330 X5=U3-X4
340 A=AO/L*(Y1-Y2)
350 IF A<AO GOTU 370
360 A=AO
370 F=1.05*FO*A/AO*(1+V1*V)
375 F=F*AO
380 R4=D*A** *(U1-U2)/144
390 M4=M4+R4*T1
400 R=R4*(U1-U2)
410 A1=- (F+R)/(M1+M4)
415 IF J=0 GOTU 420
416 A1=-F/(M1+M4)
420 U1=U1+A1*T1
430 V1=Y1+12*U1*T1
```

8.1 (CONT'D)

```

570 A2=F/(Y2+M5)
575 IF J=0 GOTO 580
576 A2=(Z+R)/(Y2+M4)
580 U2=U2+A2*T1
590 Y2=Y2+I2*U2*T1
600 IF T<N*IE-4 GOTO 670
610 PRINT USING 270,T*IE+O,-A1/G,U1,Y1,A2/G,U2,Y2,F/K,R/X
620 IF U2=>U1 GOTO 700
630 V=M*1
640 T=T*1
650 IF U2<U1 GOTO 320
660 GOTO 810
670 STOP
700 PRINT "SPRING CONSTANTS C1,C2="
710 INPUT C1,C2
720 Z1=-A1*M1/C1
730 Z2=Z1*C1/C2
740 PRINT U1,T1%e -A1
750 Y1=Y2=Y3=0
760 X1=C1-Y3+Y1
770 IF X1>0 GOTO 820
780 IF X1<=C1 GOTO 850
790 U1=U3=(M1*U1+M3*U3)/(M1+M3)
800 X2=C2-Y2+Y3
810 IF X2=0
820 IF X2<=C2 GOTO 970
830 U3=U2=(M3*U3+M2*U2)/(M3+M2)
840 X2=C2
850 A1=-Z1*X1/M1
980 A3=(Z1*X1-Z2*X2)/M3
1000 A2=Z2*X2/M2
1010 U1=U1+A1*1
1020 U2=U2+A2*T1
1030 U3=U3+A3*T1

```


8.1 (CONT'D)

```

1050 Y1=Y1+12*J1*I1
1060 Y2=Y2+12*J2*I1
1170 Y3=Y3+12*J3*I1
1140 IF I<N4 IE=4 GOTO 1220
1150 PRINT USING 280,T*1E+6,-A1/G,U1,X1,A2/G,U2,X2,A3/G,U3
1200 IF .1 GOTO 1260
1210 N=I/4.5
1220 T=I*I1
1230 IF X1+X2>0 GOTO 790
1240 N=1
1250 GOTO 1150
1260 END

```

8.2 PULSE1

PULSE1 14:16EDT 09/04/75

```

100 G1=454*32.2
110 X1=1.637/G1
120 X3=230/G1
130 PRINT #FO: V1=U UO=":
140 INPUT FO,V1,UO
150 U1=UO
160 I=I*UO
170 I=I*UO
180 X0=231.7/G1
190 K=1000
200 X2=3600/G1
220 X6=700/G1
230 A=12.36/1.44
240 D=270/G1/A/2.42*12
250 T1=2E-9
260 S=1.42/1.04
270 G=32200
280 Z3=86.420/.3308
290 PRINT TIME -A1 U1 Y1
300 W7=M0+X0/Z3*(1+X3/.3308)
310 W8=X2+X0/Z3*(1+X3/.3378)

```

F3"

R

F

Y6

U6

A6

Y2

A2

U2

Y2

F3"

R

F

Y6

U6

A6

Y2

8. 2 (CONT'D)

```

320 V=U1/UO
330 N5=M3-44
340 A=12.36/1.5*(V1-Y6)
350 IF A<12.36 GOTO 370
360 A=12.36
370 F=FD*A/12.36*(1+V1+V)
380 R4=D+A*S*(U1-U6)/144
390 U4=U4+R4*T1
400 J=R4*(U1-U6)
410 A1=-F/(M1+M5)
420 U1=U1+A1*T1
430 Y1=Y1+12*U1*T1
440 IF X3<.3308 GOTO 570
450 X3=-.3308
460 U2=U6*(M8*U2+(M4+M7)*U6)/(M4+M7+M8)
470 IF F3>F+R THEN 500
475 A2=F3/M8
477 R=D+A*S*(U1-U6)*2/144
480 A6=(F+R-F3)/(M4+M7)
485 IF A6<A2 GOTO 520
490 A6=A2=(F+R)/(M4+M7+M8)
495 GOTO 520
500 A2=F3/48
510 A6=(F+R-F3)/(M4+M7)
520 F3=Z3*X3
530 U6=U6+A6*T1
540 Y6=Y6+12*U6*T1
550 U2=U2+A2*T1
560 Y2=Y2+12*U2*T1
570 X3=Y6-Y2
580 IF T<N*IE-4 GOTO 620
585 GOTO 600
590 PRINT USING 160,T*IE+6,-A1/G,U1,Y1,A2/G,U2,Y2,A6/G,U6,Y6,F/K,R/K,F3/K
600 IF U6>U1 GOTO 650
610 M=N+1
620 I=I+1
630 IF U6<U1 GOTO 300
640 GOTO 590
650 PRINT

```

8.2 (CONT'D)

```

655 STOP
660 PRINT 'SPRING CONSTANTS C1,C2='
670 INPUT C1,C2
680 C3=X3
690 U3=U4
700 Z1=-A1-A1/2:
710 Z2=E/C2
720 PRINT 'TIME -A1 U1 X1 A2 U2 X2 A3 U3 X3 A4 U4 X4'
730 Y1=Y2*X3*Y6=0
740 Y1=C1-Y3*Y1
750 IF X1>0 GOTO 760
760 A1=0
770 GOTO 800
780 IF X1<C1 GOTO 800
790 X1=C1
800 X2=C2-Y6*Y3
810 IF X2>0 GOTO 840
820 X2=0
830 GOTO 860
840 IF X2<C2 GOTO 860
850 X2=C2
860 X3=C3-Y2*Y6
870 IF X3>0 GOTO 900
880 X3=0
890 GOTO 920
900 IF X4<=3308 GOTO 920
910 X3=3308
920 A1=-Z1*X1/H
930 X3=(Z1*X1-Z2*X2)/M3
940 A2=(Z2*X2-Z3*X3)/M1
950 U1=U1+A1*H
960 U2=U2+A2*H
970 U3=U3+A3*H
980 U6=U6+A6*H
1000 Y1=Y1+12*U1*H
1010 Y2=Y2+12*U2*H
1020 Y3=Y3+12*U3*H
1030 Y6=Y6+12*U6*H

```

8.2 (CONT'D)

```
1040 F1=Z1*X1
1050 F2=Z2*X2
1060 F3=Z3*X3
1070 IF T<N*1E-4 GOTO 1120
1080 PRINT USING 170,T*1E+6,-A1/G,U1,X1,A2/G,U2,X2,A3/G,U3,X3,A6/G,U6
1095 GOTO 1100
1099 PRINT F1/K,F2/K,F3/K
1095 PRINT Y1,Y2,Y3,Y6
1100 IF N#1 GOTO 1160
1110 N=N+.5
1120 T=T*11
1130 IF X1*X2+X3>0 GOTO 740
1140 N#1
1150 GOTO 1080
1160 END
```

8.3 PULSE3

PULSE3 14:19 EDT 09/04/75

```
100 G1=454*32.2
110 Y1=1480/G1
120 M3=260/G1
130 PRINT "FO=t V1=t U0=t"
140 INPUT F0,V1,U0
150 U1=U0
160 t=t*.99
170 t=t*.99
180 M0=2310/G1
190 K=1700
200 M2=3660/G1
210 M6=700/G1
220 A=12.56/144
230 D=270/G1/A/2.42*12
240 I1=2E-6
250 S=1.42/1.04
260 C=32200
270 Z3=86420/.3308
```

```

6.3 (CONT'D)
280 PRINT*TIME -A1 U1 Y1 F3
290 A7=A6*NO/2*(1+X3/.3308)
300 R6=R2*NO/2*(1+X3/.3308)
310 V=J1/UC
320 W5=M3-W4
330 A=12.5*O/2.65*(Y1-Y6)
340 IF A<12.5 GOTO 360
350 A=12.56
360 R=P0*A/12.56*(1+V1+V)
370 R4=D*A*S*(U1-U6)/144
380 W4=H4+R4*T1
390 R=R4*(U1-U6)
400 A1=-F/(R1+M5)
410 U1=U1+A1*T1
420 Y1=Y1+12*U1*T1
430 IF X3<.3308 GOTO 530
440 X3=.3308
450 U2=U6*(M8+U2*(M4+M7)+U6)/(M4+M7+M8)
460 R=D*A*S*(U1-U6)^2/144
470 IF F3>F+R THEN 530
480 A2=F3/M8
490 A6=(F+R-F3)/(M4+M7)
500 IF A6<A2 GOTO 550
510 A6=A2*(F+R)/(M4+M7+M8)
520 GOTO 550
530 A2=F3/M8
540 A6=(F+R-F3)/(M4+M7)
550 F3=Z3*X3
560 U6=U6+A6*T1
570 Y6=Y6+12*U6*T1
580 U2=U2+A2*T1
590 Y2=Y2+12*U2*T1
600 X3=Y6-Y2
610 IF X3>0 GOTO 630
620 X3=0
630 IF T<N*1E-4 GOTO 670
640 PRINT USING 160,T+1E+6,-A1/G,U1,Y1,A2/G,U2,Y2,A6/G,U6,Y6,F/K,R/K,F3/K
650 IF U6<=U1 GOTO 700
660 N=N+1

```

8.3 (CONT'D)

```

670 F=T+1
680 IF U6<01 GOTO 290
690 GOTO 640
700 PRINT
710 B0=24.5200/134
720 B1=-.347950986*IE+5
730 B2=-.002343053229*IE+13
740 B3=-5.648307446*IE+14
750 B4=6.0350222916*IE+16
760 B5=-3.403159277*IE+22
770 B6=1.059112463*IE+26
780 B7=-1.724018940*IE+29
790 B8=1.147970661*IE+32
800 A1=U1
810 A2=U2
820 A3=U3=(U1+U6)/2
830 M6=U6
840 C3=X3
850 T2=T
860 N1=N
870 PRINT 'C1', 'C2', 'T3'
880 INPUT C1, C2, T3
890 PRINT 'TIME' -A1 U1 X1 A2 U2 X2 A3 U3 X3 A6 U6 *
910 Y1=Y2+Y3=Y0=0
920 U1=W1
930 U2=W2
940 U3=W3
950 U6=W6
960 X1=X2=X3=T=W=0
970 N=N1
980 IF T+T2<T3 GOTO 1010
990 A1=0
1000 GOTO 1050
1010 IF T>110*IE-6 GOTO 1040
1020 A1=-.75*G*(19.96273-32.0)/110*IE+6*T+32.6)
1030 GOTO 1050
1040 A1=-.75*G*(B0+B1*T+B2*T^2+B3*T^3+B4*T^4+B5*T^5+B6*T^6+B7*T^7+B8*T^8)
1050 X1=C1-Y3*Y1

```

8.3 (CONT'D)

```

1060 IF X1>0 GOTO 1090
1070 X1=0
1080 GOTO 1120
1090 IF X1<C1 GOTO 1120
1100 U1=U3*(M1*U1+M3*U3)/(M1+M3)
1110 X1=C1
1120 X2=C2-Y6+Y3
1130 IF X2>0 GOTO 1160
1140 X2=0
1150 GOTO 1190
1160 IF X2<C2 GOTO 1190
1170 U3=U6*(M3*U3+M7*U6)/(M3+M7)
1180 X2=C2
1190 X3=C3-Y2+Y6
1200 IF X3>0 GOTO 1230
1210 X3=0
1220 GOTO 1260
1230 IF X3<-.3308 GOTO 1260
1240 U2=U6*(M9*U2+M7*U6)/(M7+M9)
1250 X3=-.3308
1260 IF X1>1E-10 GOTO 1290
1270 X1=1E-10
1280 Z1=Z2*-A1*M1/X1
1290 IF X1>.01*C1 GOTO 1310
1300 Z1=Z2*24.5*G*M1/C1
1310 A3=(Z1*X1-Z2*X2)/M3
1320 A6=(Z2*X2-Z3*X3)/M7
1330 A2=Z3*X3/M9
1340 U1=U1+A1*I1
1350 U2=U2+A2*I1
1360 U3=U3+A3*I1
1370 U6=U6+A6*I1
1380 Y1=Y1+12*U1*I1
1390 Y2=Y2+12*U2*I1
1400 Y3=Y3+12*U3*I1
1410 Y6=Y6+12*U6*I1
1420 IF (T2+T1)<N*1E-4 GOTO 1460
1430 PRINT USING 170, (T+T2)*1E+6, -A1/G, U1, X1, A2/G, U2, X2, A3/G, U3, X3, A6/G, U6
1440 N=N+.5

```

8.3 (CONT'D)

1450 IF M=1 GOTO 1500
 1460 I=T+1
 1470 IF X1+X2+X3>1*IE-8 GOTO 980
 1480 M=J
 1490 GOTO 1430
 1500 IF (I2+I)>I3+10*1*IE-6 GOTO 870
 1510 IF (I2+I)<I3-10*1*IE-6 GOTO 870
 1520 END

8.4 JMEMX

JMEMX 14*2IEDT 09/04/75

100 *****
 110 PRINT "TIME A1 U1 W A2 U2 X2 E2 X E EI F"
 120 M1=1730/32.2/454
 130 M2=15*M1
 140 M3=270/32.2/454
 150 A=12.56/144
 160 D=1270/32.2/454/A/11*12
 170 F0=1150*0
 180 T1=2E-6
 190 S=1.3
 200 G=J2200
 210 U0=U1=455
 220 E0=(M1+M3)*U0**2/2
 230 R4=D+A*S*(U1-U2)
 240 IF T<M1*IE-4 GOTO 280
 250 PRINT USING 100,T*IE+6,A1/G,U1,r,A2/G,U2,E2,X,E,EI,M4*32.2,F
 260 IF U1<=U2 GOTO 490
 270 N=N+1
 280 T=T+T1
 290 F1=F0*(1+.5*U1/U0)
 300 M4=M4+R4*T1
 310 M5=43-M4
 320 A1=-F1/(M1+M5)
 330 U1=U1+A1*T1
 340 X1=X1+12*U1*T1
 350 A2=(F1+R4*(U1-U2))/(M2+M4)


```

8.5 (CONT'D)
310 M4=M4+R4*T1
315 M5=M3-M4
320 A1=-((F1+R4*(U1-U2))/(M1+M4)
330 U1=U1+A1*T1
340 X1=X1+I2*U1*T1
350 A2=F1/(M2+M5)
360 U2=U2+A2*T1
370 X2=X2+I2*U2*T1
380 E1=M1*U6-(M1+M4)*U1-(M2+M5)*U2
385 E1=100*E1/U0
390 R=R+R4*(U1-U2)^2*T1*.5
400 W=100*R/E0
410 E2=100*((M1+M4)*U1^2+(M2+M5)*U2^2)/2/E0
420 A=X1-X2
430 F2=F2+F1*(U1-U2)*T1
440 F=107*F2/E0
450 F=100-E2-F-W
460 IF U1>U2 GOTO 237
470 GOTO 250
480 END

```

ACKNOWLEDGEMENT

It is a pleasure to acknowledge the helpful discussions and the superb computer BASIC course taught by Herbert D. Curchack of the Harry Diamond Laboratories.